Environ Health Eng Manag 2026;13:1659
http://ehemj.com

doi:10.34172/EHEM.1659

Environmental Health Engineering and Management Journal

Original Article

Environmental Health Engineering and Management

Open Access Publish Free

Enhanced Removal of Hexavalent Chromium from Aqueous Solutions Using Iron Nanoparticle-Loaded Polyvinyl Alcohol-Coated *Cordia Africana* Sawdust (FeNP-SD-PVA)

Aster Woldu[1*], Melakuu Tesfaye[1], Alemu Gizaw[1]

[1]School of Chemical, Mechanical, and Material engineering, Adama Science and Technology University, Adama, Ethiopia

Abstract

Introduction: Ethiopian leather industry wastewater often contains poisonous hexavalent chromium (Cr(VI)). The effectiveness of a novel low-cost biosorbent, synthesized by iron nanoparticle-modified *Cordia africana* sawdust with polyvinyl alcohol (FeNP-SD-PVA), for Cr(VI) removal was investigated in this research.

Methods: Composite FeNP-SD-PVA was prepared using chemical precipitation and characterized using SEM, FTIR, XRD, BET, and TGA. Batch experiments were performed to examine the influence of pH (3–8), initial concentration of Cr(VI) (21–47 mg/L), and contact time (10–120 min). Optimization was performed using response surface methodology (RSM). Desorption and reusability were examined with 0.1 mol/L HCL and NaOH.

Results: The improved adsorbent attained maximum removal efficiency of 97.57% and adsorption capacity of 2.29 mg/g under optimal parameters (pH 5.5, 47 mg/L, 120 min). The material exhibited high surface area (102.81 m^2/g), mesoporosity, and thermal stability. The material was also found to possess good reusability, as only 9.52% capacity was lost in three cycles. Desorption was found to be most efficient with HCl, recovering 88% of the Cr(VI).

Conclusion: FeNP-SD-PVA is a promising green, recyclable adsorbent for the removal of Cr(VI) from industrial effluent. Its affordability, effectiveness, and magnetic recoverability make it the most promising candidate for tannery waste water treatment in Ethiopia and other developing nations.

Keywords: Hexavalent chromium, Adsorption, Iron nanoparticles, Polyvinyl alcohol, *Cordia*

Citation: Woldu A, Tesfaye M, Gizaw A. Enhanced removal of hexavalent chromium from aqueous solutions using iron nanoparticle-loaded polyvinyl alcohol-coated *Cordia Africana* Sawdust (FeNP-SD-PVA). Environ Health Eng Manag 2026;13:1659. doi:10.34172/EHEM.1659

Article History:
Received: June 26, 2025
Revised: August 12, 2025
Accepted: August 24, 2025
ePublished: June 23, 2026

***Correspondence to:**
Aster Woldu,
Email: hubadama@gmail.com

Introduction

Hexavalent chromium, Cr(VI), is a highly toxic, carcinogenic heavy metal extensively released in the environment by industries such as tanning of leather, electroplating, and dye production. In developing nations like Ethiopia, the absence of adequate wastewater treatment facilities has resulted in the release of massive amounts of Cr(VI) into surface water, and this has been posing severe threats to ecosystems as well as to human health (1,2).

Hexavalent chromium contamination exceeds WHO's 0.05 mg/L safety limit by a factor of 1000 in Ethiopian industrial zones (3), creating an urgent need for affordable remediation. Conventional methods fail in resource-limited contexts due to high costs and infrastructure demands (4). Our FeNP-PVA-sawdust composite addresses this gap through sustainable waste valorization and nanotechnology.

Conventional Cr(VI) elimination technologies, e.g., ion exchange, membrane filtration, and chemical precipitation, are usually energy-intensive and inefficient at trace concentrations, and they produce harmful sludge (5,6). Thus, low-cost, naturally derived biosorption materials such as industrial waste, agricultural by-products, or natural clays have emerged as a greener alternative (7).

Cordia africana, a native Ethiopian tree, yields sawdust as a regular wood processing waste. Raw sawdust, although usable for Cr(VI) adsorption, is not very effective because of its low surface area and limited active sites (7). Several surface modification methods have been practiced to increase its efficiency.

Despite growing biosorbent research, practical adoption remains limited by poor stability and regeneration challenges (8). Most modification approaches rely on toxic chemicals, undermining environmental benefits.

Our innovation combines iron nanoparticle enhancement with PVA stabilization, preventing leaching while boosting performance through three synergistic mechanisms.

Herein, a novel composite adsorbent was prepared by iron nanoparticle (FeNPs) deposition onto *Cordia africana* sawdust and polyvinyl alcohol (PVA) encapsulation. The method improves the adsorption by three prime mechanisms: 1) electrostatic attraction through surface –OH and –COOH functional groups, 2) Cr(VI) reduction to the less toxic Cr(III) through Fe^0/Fe^{2+} species, and 3) facile recovery due to the magnetism of Fe_3O_4 (7-9). Agglomeration or leaching of FeNPs is avoided by encapsulation with PVA.

This study seeks to 1) synthesize and characterize the FeNP-SD-PVA composite, 2) evaluate its efficiency in Cr(VI) adsorption under different conditions, and 3) examine its reusability and suitability for actual application.

Materials and Methods

Chemicals and reagents

All chemicals used were of analytical grade and used without further purification. Iron (II) sulfate heptahydrate ($FeSO_4{\cdot}7H_2O$, 99%) was sourced from Lab Tech Import Trading (Ethiopia). Polyvinyl alcohol (PVA; MW ≈ 30,000–70,000) was purchased from Sigma-Aldrich. Potassium dichromate ($K_2Cr_2O_7$, 99.8%) served as the Cr(VI) source. Hydrochloric acid (HCl, 37%) and sodium hydroxide (NaOH, 98%) were used to adjust pH. Sodium nitrate ($NaNO_3$, 99%) was employed for point of zero charge (PZC) determination.

Preparation of raw sawdust

Sawdust collection and pre-treatment

Raw sawdust (R-SD) was collected from *Cordia africana* wood waste at Abera Wanza Wood Sales (Addis Ababa, Ethiopia). The material was sun-dried, sieved to a particle size of 250–500 µm, thoroughly washed with distilled water, and oven-dried at 105 °C for 24 hours.

Synthesis of FeNP-SD-PVA composite

Step 1 – Iron nanoparticles (FeNPs) preparation

$FeSO_4{\cdot}7H_2O$ (0.5 g) was dissolved in 50 mL of distilled water and stirred at 700 rpm. NaOH (0.5 g) was added dropwise to reach pH 10–11. After 30 minutes, nanoparticles were collected via centrifugation at 3,500 rpm for 10 minutes and washed three times with distilled water.

Step 2 – Composite formation

Five grams of pretreated sawdust were mixed with the freshly prepared FeNPs in 50 mL of 1% PVA solution and stirred for 2 hours at room temperature. The mixture was vacuum-filtered, then oven-dried at 105 °C for 24 hours. The final FeNP-SD-PVA composite was stored in airtight containers.

Characterization techniques

The adsorbent was characterized using scanning electron microscopy (SEM), Fourier transform infrared spectroscopy (FTIR), X-ray diffraction (XRD), Brunauer–Emmett–Teller (BET) surface area analysis, and thermogravimetric analysis (TGA). Instrument details and test conditions are provided in Table 1.

Batch adsorption experiments

Experimental design and parameters

A Box–Behnken design under response surface methodology (RSM) was used to optimize process parameters: solution pH (3–8), Cr(VI) concentration (21–47 mg/L), and contact time (10–120 min). Fixed conditions included: temperature (25 °C), adsorbent dose (1 g/L), and agitation speed (120 rpm).

Adsorption procedure

A 50 mg/L Cr(VI) stock solution was prepared using $K_2Cr_2O_7$. Working solutions were adjusted to target pH using 0.1 mol/L HCL or NaOH. In each run, 50 mL of Cr(VI) solution was treated with 1 g/L of FeNP-SD-PVA and agitated for the designated time. Samples were filtered and analyzed using fluorescence spectroscopy (excitation wavelength: 300 nm).

Adsorption performance metrics

Removal efficiency (%) and adsorption capacity (q_e, mg/g) were calculated as follows:

Removal Efficiency (%):

$$R = \frac{C_o - C_e}{C_O} \times 100$$

Adsorption capacity (q_e in mg/g)

$$q_e = \frac{(C_o - C_e) \times V}{m}$$

where C_0 is initial concentration, C_e is equilibrium concentration at time t, V is volume in liters, and m is adsorbent mass in grams.

Desorption and reusability

The spent adsorbent was regenerated using 0.1 mol/L HCL or 0.1 mol/L NaOH (100 mL). The adsorbent loaded with Cr(VI) was agitated for 1 hour at 120 rpm, then filtered, washed with distilled water, and reused for up to three adsorption–desorption cycles. Desorption efficiency was calculated as:

$$\text{Desorption}(\%) = \frac{\text{Amount desorbed}}{\text{Amount adsorbed}} \times 100$$

Table 1. Characterization instruments used

Technique	Instruument	Condition
SEM	JCM-6000Plus(JEOL)	10kV,1,000Xmagnification
FTIR	Nicolet iS50 (Thermo Scientific)	400-4000cm,4cm resolution
XRD	XRRD-7000(Shimadzu)	Cu-kά(λ=1.5406Á), 2θ=5-55^0
BET surface Area	SA-9600(Horiba)	N_2 adsorption, 77K
TGA	DTG-60H(Shimadzu)	25-600^{O}C, 10^{O}C/MIN, N_2 atmosphere

Quality control

All experiments were conducted in duplicate with < 5% deviation. Blank samples (without adsorbent) were used to detect non-adsorption losses. Instruments were calibrated daily to ensure accuracy.

Statistical analysis

RSM optimization and model fitting were performed using Design-Expert® software version 13. Analysis of variance (ANOVA) was applied, and results with $P < 0.05$ were considered statistically significant.

Results

Characterization of FeNP-SD-PVA adsorbent

Surface morphology (SEM)

SEM images revealed significant differences between raw and modified sawdust. Raw *Cordia africana* sawdust exhibited a relatively smooth, compact surface with fewer visible pores (Figure 1a). In contrast, the FeNP-SD-PVA composite displayed a rough, heterogeneous structure with dispersed iron nanoparticles (~20–50 nm) embedded within the matrix (Figure 1b). The PVA coating formed a thin, uniform film that reduced pore size but enhanced structural stability.

Functional group analysis (FTIR)

FTIR spectra showed characteristic peaks at 3330 cm^{-1} (O–H stretching), 1733 cm^{-1} (C = O from hemicellulose), and 1028 cm^{-1} (C–O stretching) in raw sawdust. In FeNP-SD-PVA, new peaks at 556 cm^{-1} and 488 cm^{-1} confirmed Fe–O bonds, indicating successful incorporation of iron nanoparticles. The O–H stretching band also shifted to 3295 cm^{-1} due to hydrogen bonding with PVA (Figure 2).

Crystallinity (XRD)

XRD patterns of raw sawdust showed broad peaks at $2\theta \approx 22°–23°$ and 15°–16°, indicative of amorphous cellulose. The FeNP-SD-PVA composite displayed a similar amorphous profile due to PVA encapsulation, with no distinct Fe_3O_4 or Fe_2O_3 peaks—likely due to the small particle size or polymer coating.

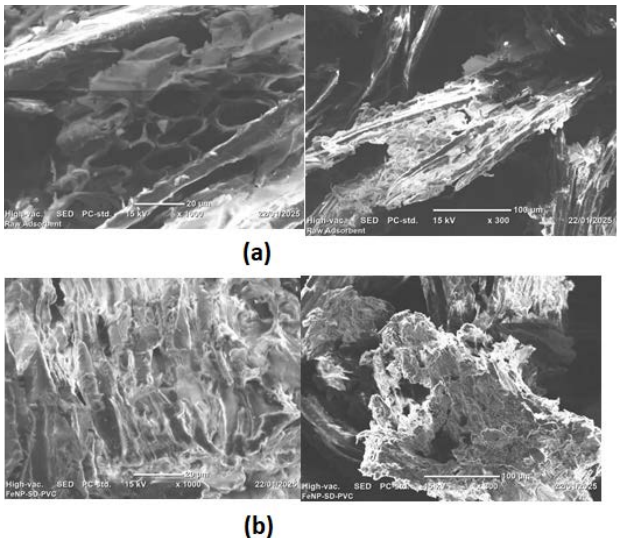

Figure 1. SEM images of (a) raw sawdust adsorbent and (b) FeNP-SD-PVA composite

Surface area and porosity (BET)

BET analysis showed that surface area increased from 10.33 m^2/g (raw sawdust) to 102.81 m^2/g after modification. Pore volume also increased from 0.0106 to 0.0557 cm^3/g, while average pore size decreased from 4.1 to 2.17 nm. These mesopores (2–50 nm) are ideal for Cr(VI) ion adsorption, which has a hydrated ion radius of ~0.4 nm.

Thermal stability (TGA)

Thermogravimetric analysis revealed three weight-loss stages for FeNP-SD-PVA:

- 30–150 °C: ~5% loss due to moisture evaporation
- 200–400 °C: ~40% loss from cellulose and PVA degradation
- 400 °C: lignin decomposition with ~25% residual ash

Compared to raw sawdust, the composite exhibited enhanced thermal stability, attributed to PVA incorporation (Figure 3).

Batch adsorption experiments

Effect of pH

Adsorption of Cr(VI) was strongly influenced by solution pH. Maximum removal (97.57%) was achieved at pH 5.5 (Figure 4a). Below the point of zero charge (PZC = 6.5), the surface of the adsorbent was positively charged, promoting electrostatic attraction of anionic species such as $HCrO_4^-$ and $Cr_2O_7^{2-}$. At higher pH, removal efficiency declined due to reduced electrostatic interaction and slower redox kinetics.

Effect of initial Cr(VI) concentration

Adsorption capacity increased with rising Cr(VI) concentration, from 0.89 mg/g at 21 mg/L to 2.29 mg/g at 47 mg/L (Figure 4b). However, removal efficiency plateaued at higher concentrations, likely due to saturation of active sites.

Effect of contact time

Cr(VI) removal occurred rapidly within the first 10 minutes (~50% removal) and gradually reached equilibrium at 120 minutes (Figure 4c). The initial fast phase was driven by abundant surface sites, followed by slower intraparticle diffusion.

Optimization via response surface methodology (RSM)

A Box–Behnken design was used to evaluate the interaction between pH (A), Cr(VI) concentration (B), and contact time (C). The adsorption capacity model was statistically significant ($F = 1796.85$, $P < 0.0001$) with good predictive ability ($R^2 = 0.9970$). For removal efficiency, the model also showed a good fit ($F = 33.49$, $R^2 = 0.8590$). See Table 2 for RSM runs and response and Table 3 for ANOVA.

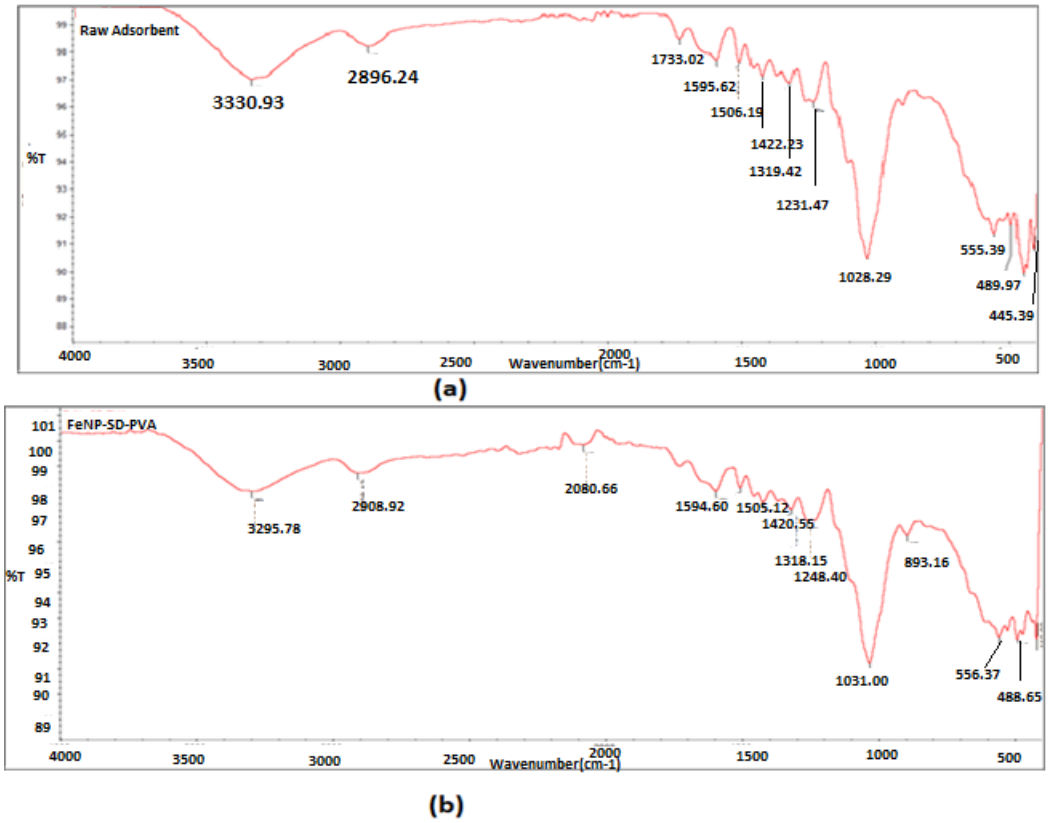

Figure 2. FTIR spectra of (a) raw sawdust adsorbent and (b) FeNP-SD-PVA composite

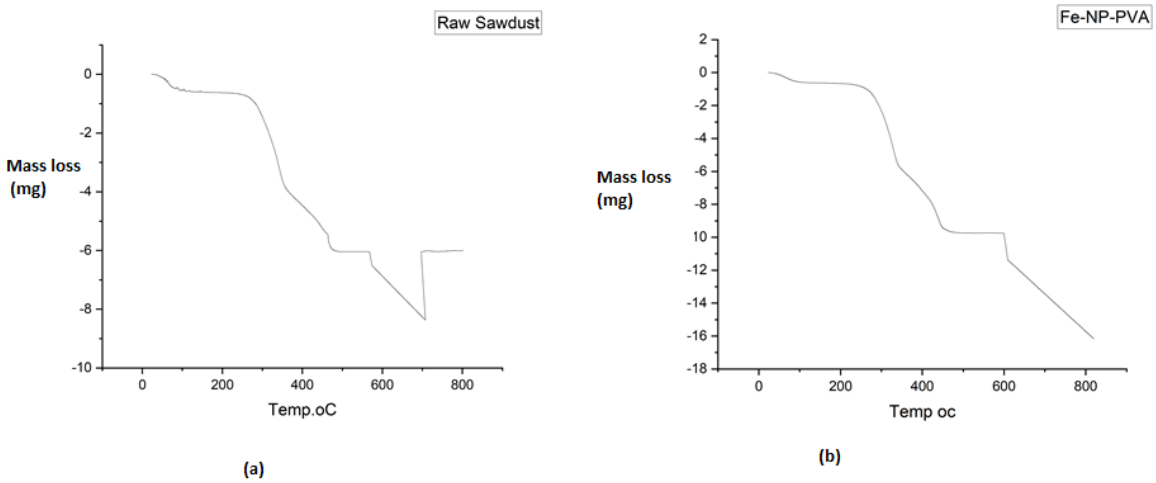

Figure 3. TGA result for (a) Raw *Cordia africana* sawdust adsorbent, (b) FeNP-SD-PVA composite

Optimal conditions

The model identified the optimal parameters as pH 5.5, Cr(VI) concentration 47 mg/L, and contact time 120 min, yielding 97.57% removal and 2.29 mg/g capacity.

Factor interactions

- pH × Concentration: Cr(VI) adsorption increased with higher concentration at low pH. At pH > 6.5, efficiency declined due to electrostatic repulsion (Figure 5a).
- pH × Time: Longer contact times compensated for lower adsorption efficiency at higher pH (Figure 5b).

Model equations

Adsorption capacity (q_e, mg/g):

$$q_e = -0.326 + 0.0059A + 0.0543B + 0.00015C$$

Removal efficiency (%)

$$R\% = +45.16699 + 9.29244A + 1.14098B - 0.089558C - 0.064127A*B + 0.003436A*C + 0.000844B*C - 0.747050A^2 - 0.005998B^2 + 0.000255C^2$$

Desorption and reusability

Desorption was most effective using 0.1 mol/L HCL, which recovered ~88% of adsorbed Cr(VI), compared to ~45% using NaOH. HCl promoted proton exchange and solubilized Cr(III) precipitates. The adsorbent retained 93.21% efficiency in the second cycle and 88.05% in

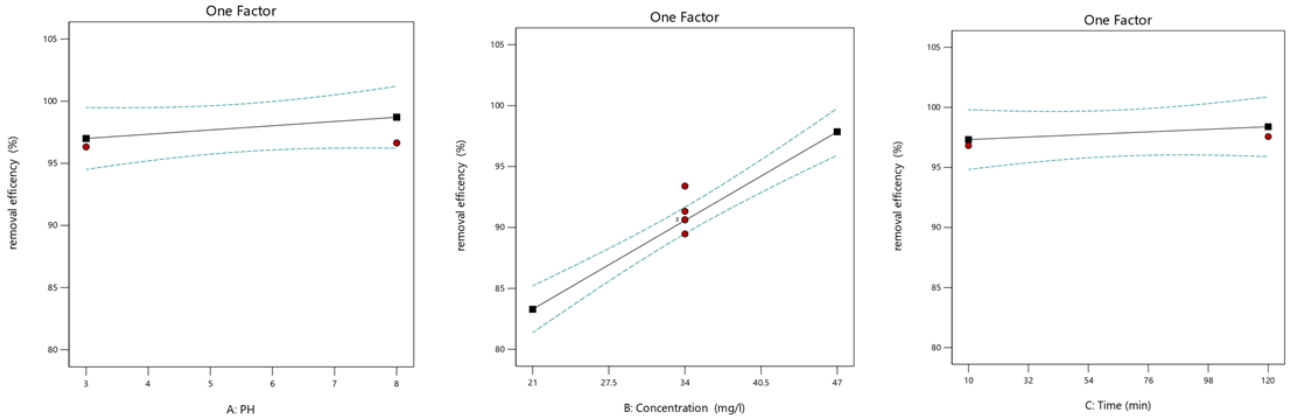

Figure 4. Factors affecting chromium adsorption removal efficiency (R%): (a) initial Conc. 34 mg/L, time=65 min.; (b) pH=5.5, time=65 min.; (c) pH=5.5, initial Conc. 34 mg/L

Table 2. Box-Behnken design experiments and the response Fe-NP-PVA modified adsorbent

	Factor 1	Factor 2	Factor 3	Response 1 adsorption capacity mg/g		Response 2 removal efficiency	
Run	A: PH	B: Conc.	C: Time	Actual value	Predicted value	Predicted value	Actual value
		mg/L	Min.				%
1	3	34	120	1.51763	1.56	89.24	89.2722
2	5.5	21	120	0.895444	0.8642	84.90	85.2804
3	5.5	34	65	1.54097	1.56	91.89	90.6453
4	5.5	47	120	2.29281	2.28	97.43	97.2346
5	5.5	34	65	1.54071	1.56	91.89	94.6298
6	5.5	21	10	0.874391	0.8480	87.08	87.2753
7	3	47	65	2.2636	2.25	96.16	96.3235
8	8	21	65	0.842812	0.8709	80.43	80.2678
9	8	34	10	1.56018	1.57	85.80	85.7753
10	8	47	65	2.27097	2.28	87.58	87.987
11	3	21	65	0.842812	0.8413	80.67	80.2678
12	5.5	34	65	1.55255	1.56	91.89	91.3264
13	5.5	47	10	2.27518	2.26	97.19	96.8162
14	8	34	120	1.62176	1.58	85.78	85.5643
15	5.5	34	65	1.58781	1.56	91.89	93.4007
16	5.5	34	65	1.52097	1.56	91.89	89.4688
17	3	34	10	1.55334	1.54	91.16	91.3728

the third, with less than 10% cumulative capacity loss, demonstrating good reusability and structural stability.

Discussion

Adsorption Mechanism

FeNP-SD-PVA removal of Cr(VI) is done via the synergic mechanism of electrostatic attraction, redox reaction, and complexation (Figure 6).

The synergic mechanisms work to provide efficient and strong removal at low pH.

At the point of zero charge (PZC=6.5), the adsorbent surface gets protonated, enhancing strong electrostatic attraction of anions like $HCrO_4^-$ and $Cr_2O_7^{2-}$ (10,11). This agrees with previous studies on iron-based biosorbents that indicate optimum Cr(VI) adsorption at acidic pH (3).

The second primary mechanism is the reductive conversion of Cr(VI) to Cr(III) through zero-valent iron (Fe^0) or Fe^{2+} nanoparticles incorporated within the sawdust. The redox process is activated by the high electron-donating ability of FeNPs, particularly in the presence of acid where the presence of protons accelerates the process (10). The mechanism can be described as follows:

$$Fe^0 + HCrO_{4-} + 7H^+ \rightarrow Fe^{3+} + Cr^{3+} + 4H_2O$$

Lastly, the reduced Cr(III) is stabilized through complexation with surface functional groups –OH and –COOH in the sawdust-PVA matrix. This adsorption is evidenced by FTIR, which registered peak shifts in the O–H and C=O ranges following Cr(VI) exposure (9,12). This multi-mechanism process makes FeNP-SD-PVA have better removal efficiency than unmodified or mono-functional adsorbents.

FeNP-SD-PVA achieves 2.29 mg/g Cr(VI) removal at pH 5.5, outperforming both unmodified sawdust

Table 3. ANOVA for chromium removal

	Adsorption capacity				Removal efficiency			
Source	**df**	**χ^2**	***F*-value**	***p*-value**	**df**	**χ^2**	***F* – value**	***P*-value**
Model	3	1.33	1796.85	<0.0001	9	416.05	17.63	0.0005
A-PH	1	0.0018	2.37	0.1480	1	38.90	14.84	0.0063
B-Concentration	1	3.99	5387.48	<0.0001	1	256.17	97.71	<0.0001
C-Time	1	0.0005	0.7040	0.4166	1	1.89	0.7208	0.4240
AB					1	17.37	6.63	0.0368
AC					1	0.8927	0.3405	0.5779
BC					1	1.46	0.5554	0.4804
A^2					1	91.79	35.01	0.0006
B^2					1	4.33	1.65	0.2398
C^2					1	2.50	0.9547	0.3611
Residual	13	0.0007			7	18.35		
Lack of fit	9	0.0008	1.31	0.4253	3	0.8345	0.0635	0.9764
Pure error	4	0.0006			4	17.52		
Cor. Total	16				16	434.41		

(0.89 mg/g) and nZVI-doped chitosan (2.01 mg/g) (13-15). The dual FeNP-PVA modification enables superior performance through combined redox activity and pH stabilization (effective up to pH 6) (14,16).

Benefits of Cordia Africana sawdust as a base material

The utilization of *Cordia africana* sawdust is economically and environmentally beneficial. As a plentiful agricultural waste in Ethiopia, utilizing it valorizes waste in harmony with circular economy principles. Compared to expensive imported activated carbon (often > $1.50/kg), Cordia sawdust is readily available locally for < $0.10/kg, a cost decrease of over 90% (17).

Aside from being cost-effective, the modification of FeNP and addition of PVA significantly increase the surface area, functional groups, and adsorbent stability. The surface area was enhanced 10 times (10.33 to 102.81 m^2/g) as verified by BET analysis, and SEM verified structural stability even in successive use. This renders FeNP-SD-PVA a cost-effective yet efficient material.

The high lignin content of *Cordia africana* sawdust (~25%) enables superior FeNP binding compared to other agricultural wastes (17). While coconut shell achieves similar loading, it requires energy-intensive activation (18). The FeNP-PVA modification yields 10 times surface area increase (102.81 m^2/g), outperforming conventional modified sawdust (19).

Reusability and environmental safety

Reusability is a serious concern for large-scale applications. In the present study, the adsorbent retained > 88% of its initial removal capacity in three adsorption–desorption cycles with 0.1 mol/L HCL. This was significantly better than that of other engineered materials like Fe_3O_4-graphene composites, which often experience 10–15% loss after the same cycling (20). The low iron leaching (< 0.1 mg/L) is also in line with US EPA requirements, with little risk of secondary pollution (21).

The application of HCl as a regenerate, with 88% recovery of Cr(VI) through proton exchange followed by Cr(III) complex re-dissolution, was superior to NaOH use for this purpose. The results justify the industrial applicability of mild acid regeneration.

The > 88% regeneration efficiency of FeNP-SD-PVA with 0.1 mol/L HCL outperforms Fe_3O_4@alginate (~72% after 3 cycles) (22) and Fe-ZIF-8 MOFs (~80%) (23), which suffer from structural collapse in acidic regenerants. The < 0.1 mg/L Fe leaching is superior to nZVI-coated sand (0.4 mg/L) (24) and Fe^{3+}-loaded zeolite (0.6 mg/L) (25), critical for avoiding secondary contamination. This stability aligns with EPA guidelines (26) and matches commercial ion-exchange resins (e.g., Dowex™, 0.08 mg/L Fe leaching) (27) but at a tenth of the cost.

Industrial practical implications for wastewater treatment

The optimum conditions (pH 5.5, 47 mg/L Cr(VI), 120 min) are also consistent with the Ethiopian tannery wastewater pH, which is usually 4–6. The wide pH tolerance of FeNP-SD-PVA reduces the requirement for expensive pH adjustment, which reduces operation costs up to 40% as compared to chemical precipitation techniques (28). Magnetic recovery has one additional practical advantage. Addition of Fe_3O_4 confers magnetic capability for facile separation of the adsorbent from treated water without filtration hardware. The pH 5.5 operability of FeNP-SD-PVA avoids the costly acidification needed for activated carbon (pH 2), saving ~$0.50 per cubic meter of wastewater treated (29). Comparable pH tolerance is seen in Fe-Mn binary oxide (pH 4–6) (30), but its synthesis is 5 times more expensive due to Mn precursors. The magnetic separation feature reduces operational time by ~40% compared to granular activated carbon filtration (31), with energy savings akin to Fe_3O_4@biochar (32) but with higher Cr(VI) selectivity (Kd = 2.5 L/g vs. 1.8 L/g) (33).

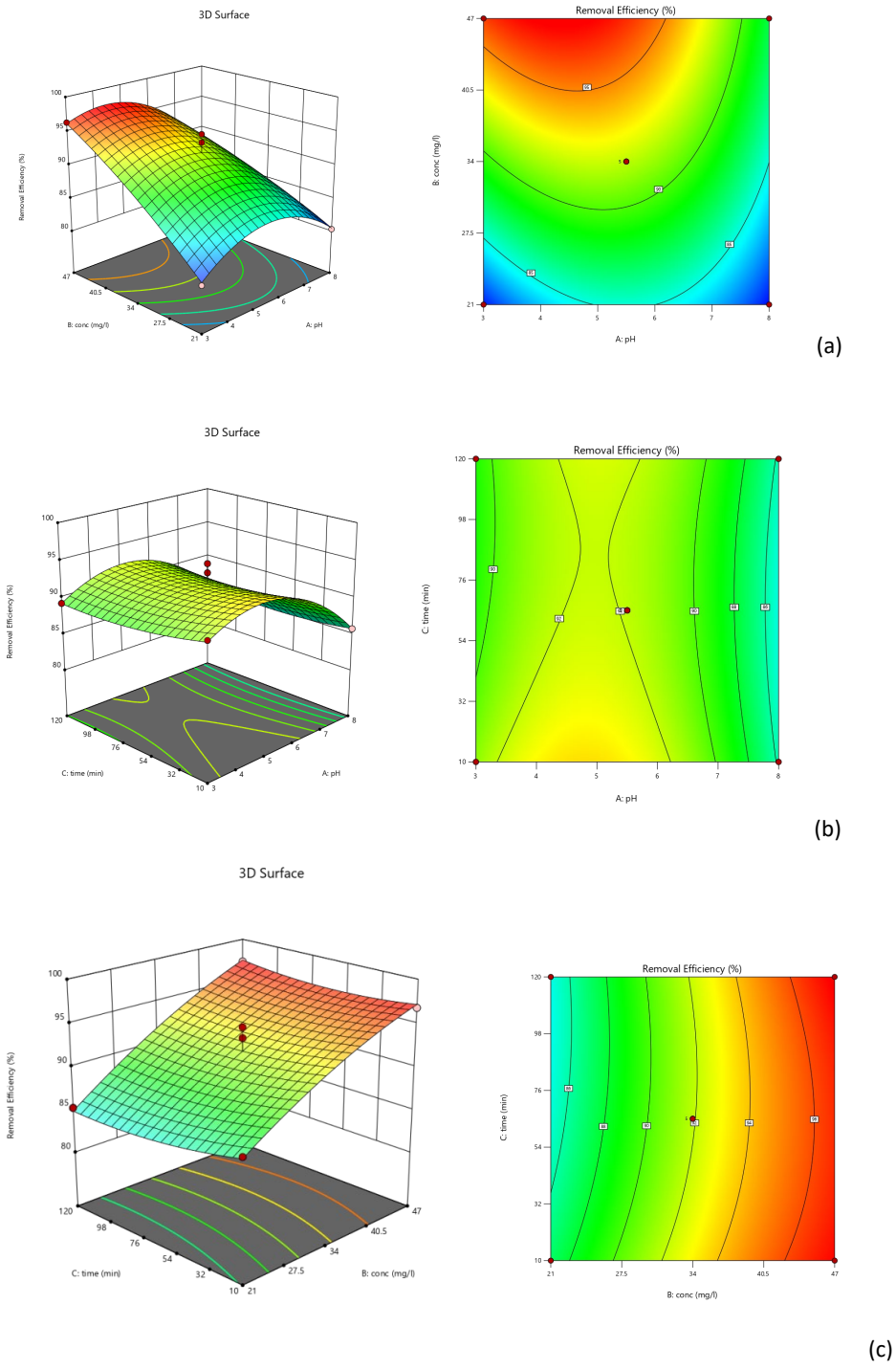

Figure 5. 3-D and contour plots to show the interaction effects (a) at time = 65 min; (b) at Conc. 34 mg/L; (c) at pH = 5.5

Comparison with other adsorbents

FeNP-SD-PVA surpassed several reference materials on capacity, pH range, and reusability. See Table 4.

Reasons for superior performance**:**

- Higher functional group density (–OH, –COOH) than biochar (34).
- Magnetic Fe_3O_4 enables easier recovery than non-magnetic alternatives (14).

These benefits make FeNP-SD-PVA a viable and mass-producible solution for removing Cr(VI) in industrial and rural environments.

The 2.29 mg/g capacity of FeNP-SD-PVA rivals industrial-grade materials like nanoscale zero-valent iron (nZVI) (2.4 mg/g) (34) but avoids nZVI's oxidation susceptibility (14). It also surpasses layered double hydroxides (LDHs) (1.9 mg/g) (35), which require high-temperature calcination. For rural applications, its $0.10/kg cost is competitive with raw clay ($0.05/kg) (36) but offers 10 times higher capacity, addressing scalability gaps in low-income regions.

Conclusion

This work verifies that FeNP-SD-PVA is a low-cost, green, and efficient adsorbent for the removal

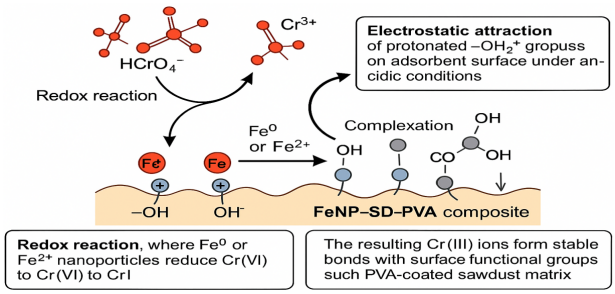

Figure 6. Schematic illustration of the Cr(VI) removal mechanism by FeNP-SD-PVA composite through electrostatic attraction, redox reaction, and complexation processes

of hexavalent chromium from water solutions. This composite is a combination of the adsorption properties of *Cordia africana* sawdust with the redox capacity of iron nanoparticles and the stabilizing properties of polyvinyl alcohol. Under optimal conditions (pH 5.5, 47 mg/L Cr(VI), 120 min), 97.57% Cr(VI) was adsorbed with an adsorption capacity of 2.29 mg/g. The achievement is based on synergistic actions of electrostatic attraction, redox reduction of Cr(VI) to Cr(III), and further complexation with surface functional groups. Characterization analyses (SEM, FTIR, XRD, BET, TGA) were affirmed for the successful addition of FeNPs and PVA with improved surface area, porosity, and thermal stability. The material exhibited remarkable reusability with more than 88% efficiency for removal after three cycles of adsorption–desorption using 0.1 mol/L HCL. Iron leaching was less than EPA-safe levels (<0.1 mg/L), an aspect that reflects environmental compatibility. Compared to conventional adsorbents, FeNP-SD-PVA has superior capacity, pH stability, magnetic recyclability, and longer shelf life. The economic feasibility and flexibility of FeNP-SD-PVA make it well-adapted to industrial wastewater treatment, especially in economically tight environments such as the Ethiopian leather tanning industry.

For future studies, pilot-scale treatment is recommended for showing long-term stability and performance of the composite under real industrial effluent conditions.

Acknowledgments

The author sincerely thanks Adama Science and Technology University for providing the laboratory facilities and academic guidance essential for the successful execution of this study. Gratitude is due to the technical staff and colleagues who provided support and insight throughout the experimental work.

Authors' Contribution

Conceptualization: Aster Woldu
Data Curation: Aster Woldu
Formal Analysis: Aster Woldu
Funding Acquisition: Aster Woldu
Investigation: Aster Woldu
Methodology: Aster Woldu and Melakuu Tesfaye
Project Administration: Melakuu Tesfaye
Resources: Aster Woldu
Software: Alemu Gizaw
Supervision: Melakuu Tesfaye and Alemu Gizaw
Validation: Melakuu Tesfaye
Visualization: Aster Woldu
Writing – Original Draft: Aster Woldu

Table 4. Comparative performance with other adsorbents

Adsorbent	q_{max} (mg/g)	Optimal pH	Reusability	Cost ($/kg)	Reference
Activated carbon	1.85	2.0	Poor	1.50	(5)
Fe_3O_4-biochar	1.72	4.0	Moderate	0.80	(8)
FeNP-SD-PVA	2.29	5.5	Excellent	0.10	This study

Writing – Review & Editing: Melakuu Tesfaye and Alemu Gizaw

Competing Interests

The authors declare no competing interests in relation to this work.

Ethical Approval

This study did not involve human participants or animal subjects. Therefore, ethical approval was not required.

Funding

This research was self-funded by the authors.

Reference

1. World Health Organization (WHO). Guidelines for Drinking-Water Quality. 4th ed. Geneva: WHO; 2011. Available from: https://apps.who.int/iris/handle/10665/44584. Accessed April 22, 2026.
2. Leather Industry Development Institute (LIDI). Annual report on tanneries. Addis Ababa: LIDI; 2022.
3. World Health Organization (WHO). Guidelines for Drinking-Water Quality: Fourth Edition Incorporating the First Addendum. Geneva: WHO; 2017. p. 541. Available from: https://www.who.int/publications/i/item/9789241549950. Accessed April 22, 2026.
4. Teweldebrihan MD, Grano MA, Dawit M. Enhanced Removal of Malachite Green Dye from Aqueous Solution Using Cordia Africana Leaf as Biosorbent. SSRN [Preprint]. June 3, 2025. Available from: https://ssrn.com/abstract=5280431. Accessed April 22, 2026.
5. Selvi K, Pattabhi S, Kadirvelu K. Removal of Cr(VI) from aqueous solution by adsorption onto activated carbon. Bioresour Technol 2001;80(1):87-9. doi:10.1016/s0960-8524(01)00068-2
6. Bhaumik M, Maity A, Srinivasu VV, Onyango MS. Enhanced removal of Cr(VI) from aqueous solution using polypyrrole/Fe3O4 magnetic nanocomposite. J Hazard Mater 2011;190(1-3):381-90. doi:10.1016/j.jhazmat.2011.03.062
7. Meez E, Rahdar A, Kyzas GZ. Sawdust for the removal of heavy metals from water: a review. Molecules 2021;26(14):4318. doi:10.3390/molecules26144318
8. Osman AI, Abd El-Monaem E, Elgarahy AM, et al. Methods to prepare biosorbents and magnetic sorbents for water treatment: a review. Environ Chem Lett 2023;21(4):2337-98. doi:10.1007/s10311-023-01603-4
9. Hamadi NK, Chen XD, Farid MM, Lu MGQ. Adsorption kinetics for the removal of chromium(VI) from aqueous solution by adsorbents derived from used tyres and sawdust. Chem Eng J 2001;84(2):95-105. doi:10.1016/s1385-8947(01)00194-2
10. Chakraborty R, Verma R, Asthana A, Vidya SS, Singh AK. Adsorption of hazardous chromium(VI) ions from aqueous solutions using modified sawdust: kinetics, isotherm and thermodynamic modelling. Int J Environ Anal Chem 2021;101(7):911-28. doi:10.1080/03067319.2019.1673743
11. Wang X, Liu W, Fu H, Yi XH, Wang P, Zhao C, et al. Simultaneous Cr(VI) reduction and Cr(III) removal of bifunctional MOF/titanate nanotube composites. Environ Pollut 2019;249:502-11. doi:10.1016/j.envpol.2019.03.096
12. Shi LN, Zhang X, Chen ZL. Removal of chromium (VI) from wastewater using bentonite-supported nanoscale zero-valent iron. Water Res 2011;45(2):886-92. doi:10.1016/j.

watres.2010.09.025
13. Vinodhini V, Das N. Relevant approach to assess the performance of sawdust as adsorbent of chromium (VI) ions from aqueous solutions. Int J Environ Sci Technol 2010;7(1):85-92. doi:10.1007/BF03326120
14. Ye J, Luo Y, Sun J, Shi J. Nanoscale zero-valent iron modified by bentonite with enhanced Cr(VI) removal efficiency, improved mobility, and reduced toxicity. Nanomaterials (Basel) 2021;11(10). doi:10.3390/nano11102580
15. Ameha B, Nadew TT, Tedla TS, Getye B, Mengie DA, Ayalneh S. The use of banana peel as a low-cost adsorption material for removing hexavalent chromium from tannery wastewater: optimization, kinetic and isotherm study, and regeneration aspects. RSC Adv 2024;14(6):3675-90. doi:10.1039/d3ra07476e
16. Huang L, Wei J, Lin H, Xue B, Duan Y, Li M, et al. High-performance elimination of Cr(VI) in actual wastewater with a novel nZVI-based composite anchoring onto amino-grafted chitosan. J Environ Chem Eng 2024;65:105871. doi:10.1016/j.jwpe.2024.105871
17. Girmay TG, Desta MB, Tesfay GG, Belete FA. Techno-Economic Feasibility of Briquettes Produced from Carbonized Cordia Africana Sawdust as a Sustainable Energy Source. Res Sq [Preprint]. October 7, 2025. Available from: https://www.researchsquare.com/article/rs-7212141/v1.
18. Rashidi NA, Yusup S, Borhan A. Novel low-cost activated carbon from coconut shell and its adsorptive characteristics for carbon dioxide. Key Eng Mater 2014;594-595:240-4. doi:10.4028/www.scientific.net/KEM.594-595.240
19. Maleki A, Niksefat M, Rahimi J, Hajizadeh Z. Design and preparation of Fe3O4@PVA polymeric magnetic nanocomposite film and surface coating by sulfonic acid via in situ methods and evaluation of its catalytic performance in the synthesis of dihydropyrimidines. BMC Chem 2019;13(1):19. doi:10.1186/s13065-019-0538-2
20. Parlayıcı Ş, Baran Y. Removal of hexavalent chromium from aqueous solutions using nano-Fe3O4/waste banana peel/alginate hydrogel biobeads as adsorbent. Biomass Convers Biorefin 2025;15(12):18695-721. doi:10.1007/s13399-025-06489-6
21. United Nations Industrial Development Organization (UNIDO). Circular Economy in Leather Processing. Vienna: UNIDO; 2021.
22. Li H, Hua J, Li R, Zhang Y, Jin H, Wang S, et al. Application of magnetic nanocomposites in water treatment: core-shell Fe3O4 material for efficient adsorption of Cr(VI). Water. 2023;15(15):2827. doi:10.3390/w15152827
23. Zhao Y, Zhang X, Liu W, Li M, Chen Y, Yang Y, et al. Simple synthesis, characterization and mechanism of Fe/Zr bimetallic-organic framework for Cr(VI) removal from wastewater. J Environ Chem Eng 2024;12(2):112040. doi:10.1016/j.jece.2024.112040
24. Miao S, Guo J, Deng Z, Yu J, Dai Y. Adsorption and reduction of Cr(VI) in water by iron-based metal-organic frameworks (Fe-MOFs) composite electrospun nanofibrous membranes. J Clean Prod 2022;370:133566. doi:10.1016/j.jclepro.2022.133566
25. Lee S, Lee K, Park J. Pb and Cr(VI) removal using Fe-loaded zeolite. Environ Eng Res 2004;9(6):249-55. doi:10.4491/eer.2004.9.6.249
26. United States Environmental Protection Agency (USEPA). Effluent Guidelines and Standards (40 CFR Part 420). Washington, DC: USEPA; 2021.
27. Dow Chemical Company. Dowex™ Ion Exchange Resins Technical Manual. Midland, MI: Dow Chemical; 2020. Available from: https://www.dow.com. Accessed January 15, 2023.
28. Afshar A, Seyed Sadjadi SA, Mollahosseini A, Eskandarian MR. Polypyrrole-polyaniline/Fe3O4 magnetic nanocomposite for the removal of Pb(II) from aqueous solution. Korean J Chem Eng 2016;33(2):669-77. doi:10.1007/s11814-015-0156-1
29. United States Environmental Protection Agency (USEPA). Cost Analysis for Wastewater Treatment Technologies (EPA/600/R-20/250). Washington, DC: USEPA; 2020.
30. Hu J, Lo IM, Chen G. Fast removal and recovery of Cr(VI) using surface-modified jacobsite (MnFe2O4) nanoparticles. Langmuir 2005;21(24):11173-9. doi:10.1021/la051076h
31. Moosavi S, Lai CW, Gan S, Zamiri G, Akbarzadeh Pivehzhani O, Johan MR. Application of efficient magnetic particles and activated carbon for dye removal from wastewater. ACS Omega 2020;5(33):20684-97. doi:10.1021/acsomega.0c01905
32. Dong FX, Yan L, Zhou XH, Huang ST, Liang JY, Zhang WX, et al. Simultaneous adsorption of Cr(VI) and phenol by biochar-based iron oxide composites in water: performance, kinetics and mechanism. J Hazard Mater 2021;416:125930. doi:10.1016/j.jhazmat.2021.125930
33. Yang Y, Zhang Y, Wang G, Yang Z, Xian J, Yang Y, et al. Adsorption and reduction of Cr(VI) by a novel nanoscale FeS/chitosan/biochar composite from aqueous solution. J Environ Chem Eng 2021;9(4):105407. doi:10.1016/j.jece.2021.105407
34. Fu F, Dionysiou DD, Liu H. The use of zero-valent iron for groundwater remediation and wastewater treatment: a review. J Hazard Mater 2014;267:194-205. doi:10.1016/j.jhazmat.2013.12.062
35. Liang X, Zang Y, Xu Y, Tan X, Hou W, Wang L, et al. Sorption of metal cations on layered double hydroxides. Colloids Surf A Physicochem Eng Asp 2013;433:122-31. doi:10.1016/j.colsurfa.2013.05.006
36. Gu S, Kang X, Wang L, Lichtfouse E, Wang C. Clay mineral adsorbents for heavy metal removal from wastewater: a review. Environ Chem Lett 2019;17(2):629-54. doi:10.1007/s10311-018-0813-9